V. Conclusions

A general linear relationship between the coefficients of two different subblock transformations was developed. This relationship holds for any mix of linear, invertible transforms and separable subblock transform geometries (as illustrated in Fig. 1). The relationship can be found by simply precomputing the result of an inverse transform matrix multiplied by a differing forward transform matrix.

This result is a generalization of previous work by Jiang and Feng [2]. In that paper, it was also shown that the matrix giving their linear relation is sparse (which results in reduced computational load). This property holds for the DCT case when the subblocks are $A:1$ ratios of the larger blocks. In general (i.e., for other transforms and subblock ratios), this sparseness may not be present. This means that the reduction in computational load may not be as great. Whether it is efficient to relate transform coefficients by the method developed here will depend on the particular scenario as well as the applicability of any fast algorithms for the transforms of interest (these algorithms may make relating the coefficients through an inverse transform operation followed by a forward transform operation more desirable).

References

[1] G. Strang, "The discrete cosine transform," *SIAM Rev.*, vol. 41, no. 1, pp. 135–147, 1999.

[2] J. Jiang and G. Feng, "The spatial relationship of DCT coefficients between a block and its subblocks," *IEEE Trans. Signal Processing*, vol. 50, pp. 1160–1169, May 2002.

[3] J. R. Smith and S. F. Chang, "Transform feature for texture classification and discrimination in large image databases," in *Proc. 11th Int. Conf. Image Process.*, vol. 3, 1994, pp. 407–411.

[4] B. Shen and I. K. Sethi, "Direct feature extraction from compressed images," *Proc. SPIE, Storage Retrieval Image Video Databases IV*, vol. 2670, 1996.

[5] R. Reeve, K. Kubik, and W. Osberger, "Texture characterization of compressed aerial images using DCT coefficients," *Proc. SPIE, Storage Retrieval Image Video Databases V*, vol. 3022, pp. 398–407, Feb. 1997.

[6] J. R. Hernandez, M. Amado, and F. P. Gonzalez, "DCT-domain watermarking techniques for still images: detector performance analysis and a new structure," *IEEE Trans. Image Processing*, vol. 9, pp. 55–68, Jan. 2000.

[7] J. B. Lee and A. Eleftheriadis, "2-D transform-domain resolution translation," *IEEE Trans. Circuits Syst. Video Technol.*, vol. 10, pp. 704–714, Aug. 2000.

[8] J. B. Lee and B. G. Lee, "Transform domain filtering based on pipelining structure," *IEEE Trans. Signal Processing*, vol. 40, pp. 2061–2064, Aug. 1992.

[9] A. K. Jain, *Fundamentals of Digital Image Processing*. Englewood Cliffs, NJ: Prentice-Hall, 1989.

[10] I. Daubechies, *Ten Lectures on Wavelets*. Philadelphia, PA: SIAM, 1992.

A Low-Complexity Adaptive Echo Canceller for xDSL Applications

Shou-Sheu Lin and Wen-Rong Wu

***Abstract*—A finite impulse response (FIR)-based adaptive filter structure is proposed for echo cancellation in xDSL applications. The proposed algorithm consists of an FIR filter, a cascaded interpolated FIR filter, and a tap-weight overlapping and nulling scheme. This filter requires low computational complexity and inherits the stable characteristics of the conventional FIR filter. Simulations show that the proposed echo canceller can effectively cancel the echo up to 73.4 dB [for a single-pair high-speed digital subscriber line (SHDSL) system]. About 55% complexity reduction can be achieved compared with a conventional FIR filter.**

***Index Terms*—Adaptive filter, DSL, echo cancellation, interpolated FIR filter.**

I. Introduction

In a digital subscriber loop (DSL) environment, full duplex transmission via a single twisted pair can be achieved using a hybrid circuit. Due to the impedance mismatch problem, the hybrid circuit will introduce echoes. A typical echo response, shown in Fig. 1, consists of a short and rapidly changing head echo and a long and slowly decaying tail echo. Conventionally, an adaptive transversal FIR filter [1] is used to synthesize and cancel the echo. For high-speed applications such as HDSL [2], HDSL2 [3], and single-pair high-speed digital subscriber line (SHDSL) [4], the echo response is usually very long. The conventional FIR echo canceller may require hundreds of tap weights, and the computational complexity becomes very high.

In order to reduce the computational complexity, some researchers tried to use an adaptive infinite impulse response (IIR) filter to cancel the tail echo. However, the adaptive IIR filtering suffers from the local minima and stability problems. Since an IIR filter usually consists of a feedforward and a feedback filter, a compromising approach is to let the feedforward filter be adaptive only. In [5], August *et al.* collected some echo responses for the European subscriber loops and used a criterion to determine the feedback filter optimally. In [6], Gordon *et al.* considered echo cancellation as a series expansion problem. They used a set of IIR orthonormal functions to expand the echo response and let the expanding coefficients be adaptive. The orthonormal responses were obtained using a set of predetermined cascaded feedback filters. If only a small number of loops are considered, good performance can be obtained using these methods. However, since the existing loop responses are versatile, it will be difficult to find a feedback filter that will always yields the optimal performance.

To retain the FIR structure of the echo canceller, and to reduce the complexity, an interesting echo canceller structure was proposed in [7]. The canceller is cascaded from an adaptive FIR head echo canceller and an adaptive interpolated FIR (IFIR) tail echo canceller. Since the tail echo always decays smoothly, an IFIR filter with a small number of coefficients can effectively cancel the echo. Unfortunately, the IFIR filter proposed in [7] has an uncontrollable transient response, and the direct cascade of an FIR and an IFIR filter will leave a certain period of the echo response uncancelled. Although this problem is critical,

Manuscript received May 30, 2003; revised June 23, 2003. The associate editor coordinating the review of this manuscript and approving it for publication was Prof. Xiaodong Wang.

The authors are with the Department of Communication Engineering, National Chiao-Tung University, HsinChu 30050, Taiwan, R.O.C. (e-mail: gii.cm84g@nctu.edu.tw; wrwu@cc.nctu.edu.tw).

Digital Object Identifier 10.1109/TSP.2004.826155

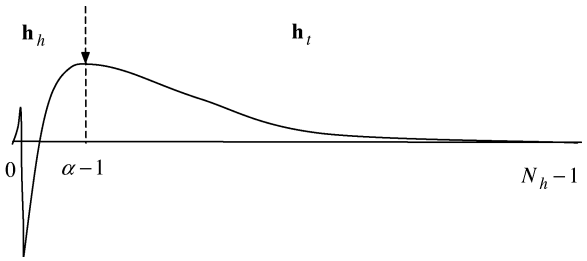

Fig. 1. Typical echo response.

it was overlooked in [7]. The authors only measured the cancellation performance of the tail echo and assumed that the remaining echo was cancelled perfectly.

In this paper, we propose a new adaptive echo canceller to remedy the problem mentioned above. In our work, the FIR and the IFIR filters are overlapped instead of being directly cascaded. Due to this overlapping operation, some echo responses will be simultaneously cancelled by the FIR and IFIR filters. Although this will not affect the final performance, it will slow down the convergence. In order to solve the problem, some of tap-weights used in the FIR filter coefficients are nulled. We call this scheme coefficient nulling. After properly nulling certain tap weights of the FIR filter, we obtain a low-complexity yet high-performance echo canceller. We also derive the corresponding Wiener solutions, the minimum mean square error (MMSE), and the error return loss enhancement (ERLE).

This paper is organized as follows. In Section II, we describe the proposed adaptive echo canceller structure and analyze the complexity in detail. In Section III, we derive the Wiener solutions, MMSE, and ERLE of the proposed algorithm. In Section IV, we show the simulation results and evaluate the validity of the derived expressions. Finally, we draw our conclusions in Section V.

II. Proposed Echo Canceller

Let the length of an echo response be N_h and its response be $\mathbf{h} = [h_0\, h_1 \ldots h_{N_h-1}]^T$. The received echo signal can be described as follows:

$$y_k = \mathbf{h}^T \mathbf{x}_k + n_k \tag{1}$$

where $\mathbf{x}_k = [x_k\ x_{k-1} \ldots x_{k-N_h+1}]^T$ is the transmitted signal, and n_k is a zero-mean additive white Gaussian noise (AWGN).

From Fig. 1, we can clearly see that a typical echo response has a fast changing head echo and a slowly varying tail echo. Thus, we can select a cutting point to segment these two portions. Let $\mathbf{h}_h = [h_0 \ldots h_{\alpha-1}]^T$, $\mathbf{x}_h = [x_k \ldots x_{k-\alpha+1}]^T$, $\mathbf{h}_t = [h_\alpha \ldots h_{N_h-1}]^T$, and $\mathbf{x}_t = [x_{k-\alpha} \ldots x_{k-N_h+1}]^T$. Then, the echo response can be re-expressed as

$$y_k = \mathbf{h}_h^T \mathbf{x}_h + \mathbf{h}_t^T \mathbf{x}_t + n_k. \tag{2}$$

In absence of noise, y_k can be synthesized and cancelled by an N_h-tap FIR filter. This filter, having $\mathbf{h}$ as its response, can be decomposed to an α-tap and an $(N_h-\alpha)$-tap FIR filter, where one cancels the head echo, and the other cancels the tail echo. In general, $(N_h-\alpha)$ is much larger than α. As a result, the tail echo canceller will dominate the overall computational complexity. Since the tail echo is slowly varying, we can use a filter with a lower complexity to approximate $\mathbf{h}_t$. The idea is to use an IFIR filter, which is an interpolation filter cascaded by a filter with an upsampled response [8]. The detailed structure of the proposed algorithm is shown in Fig. 2. The FIR filter $\mathbf{w}_1$ is used to model the head echo response $\mathbf{h}_h$ and the IFIR filter $\mathbf{g} * \mathbf{w}_2^U$, where "$*$" denotes the convolution operation and is used

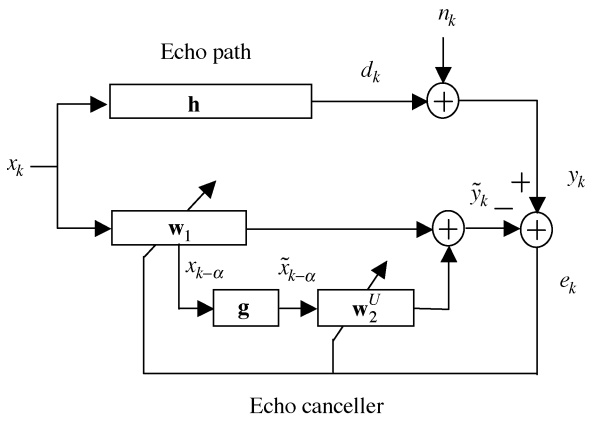

Fig. 2. Adaptive FIFIR echo canceller.

to model $\mathbf{h}_t$. Note that $\mathbf{w}_2^U$ is an upsampled version of a filter $\mathbf{w}_2$. Basically, $\mathbf{w}_2$ tries to model the downsampled version of $\mathbf{h}_t$, and $\mathbf{g}$ is a FIR filter that interpolates $\mathbf{w}_2$. Let the downsampling factor be M and the FIR filter and the IFIR filter be overlapped for $N_o = N_g - M$ taps. The head echo canceller length is extended to $N_1 = \alpha + N_o$ instead of just α. As Fig. 2 shows, x_k is the input to $\mathbf{w}_1$, and $\tilde{x}_k$ is that to $\mathbf{w}_2^U$. The output of the proposed echo canceller in Fig. 2 can be expressed as

$$\tilde{y}_k = \mathbf{w}_1^T \mathbf{x}_{1,k} + \mathbf{w}_2^T \tilde{\mathbf{x}}_{2,k} \tag{3}$$

where $\mathbf{w}_1 = [\mathbf{w}_{1,0}\ \mathbf{w}_{1,1}\ \cdots\ \mathbf{w}_{1,N_1-1}]^T$ is the N_1-tap head echo canceller, $\mathbf{x}_{1,k} = [x_k\ x_{k-1}\ \cdots\ x_{k-N_1+1}]^T$ is its input vector, $\mathbf{w}_2 = [\mathbf{w}_{2,0}\ \mathbf{w}_{2,1}\ \cdots\ \mathbf{w}_{2,N_2-1}]^T$ is the N_2-tap tail echo canceller, and $\tilde{\mathbf{x}}_{2,k} = [\tilde{x}_{k-\alpha}\ \tilde{x}_{k-\alpha-M}\ \cdots\ \tilde{x}_{k-\alpha-(N_2-1)M}]^T$ is its input vector. In terms of z-transform representation, we have $\mathbf{w}_2^U(z) = \mathbf{w}_2(z^{-M})$.

Rewriting (3), we have

$$\begin{aligned}\tilde{y}_k &= \begin{bmatrix}\mathbf{w}_1^T & \mathbf{w}_2^T\end{bmatrix}\begin{bmatrix}\mathbf{x}_{1,k}\\ \tilde{\mathbf{x}}_{2,k}\end{bmatrix}\\ &= \mathbf{w}^T \tilde{\mathbf{x}}_k.\end{aligned} \tag{4}$$

Let $\mathbf{g} = [g_0\ g_1\ \cdots\ g_{N_g-1}]^T$ be an N_g-tap interpolation filter; its length equals $2SM-1$, where S is the number of $\mathbf{w}_2$ tap-weights involved in calculating an interpolated value for a single side span. Then, the interpolator output can be expressed as follows:

$$\tilde{x}_k = \sum_{i=0}^{N_g-1} g_i x_k - i. \tag{5}$$

Generally, the impulse response of the interpolation filter $\mathbf{g}$ is peaking at the center, slowly decaying to its two sides, and is symmetric around the center. The simplest response of $\mathbf{g}$ is a triangular window function with $2M-1$ taps, which gives a linear interpolation result. Since the impulse response of IFIR filter is the convolution of $\mathbf{g}$ and $\mathbf{w}_2^U$, it exhibits two transient responses, each one decaying to zero (each with N_o samples), with one in the front end of $\mathbf{g} * \mathbf{w}_2^U$ and the other in the tail end. Since the tail end of $\mathbf{h}_t$ always decays to zero, there is no problem with that transient response in the tail. However, the head portion of $\mathbf{h}_t$ has an abrupt rising edge. As a consequence, the front-end transient response of $\mathbf{g} * \mathbf{w}_2^U$ cannot model that of $\mathbf{h}_t$. A simple way to solve this problem is to increase the length of $\mathbf{w}_1$ and overlap $\mathbf{w}_1$ with the front-end transient response of $\mathbf{g} * \mathbf{w}_2^U$. Here, we overlap the last N_o taps of $\mathbf{w}_1$ with the first N_o taps of $\mathbf{g} * \mathbf{w}_2^U$ to cover the full front-end transient response. Fig. 3 shows how the FIR and IFIR responses are overlapped. Note that in the structure, there are $(S-1)$ echo samples being cancelled

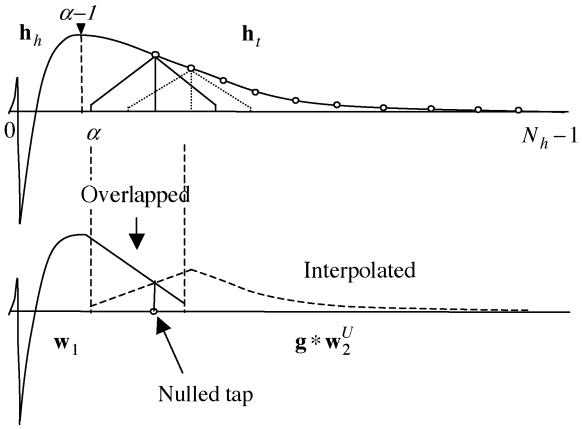

Fig. 3. Filter responses of the proposed FIFIR echo canceller.

TABLE I
COMPUTATIONAL COMPLEXITY COMPARISON FOR THE FIR AND FIFIR FILTERS

	Echo emulation		Taps weight update	
Operation	+	×	+	×
FIR	N_h-1	N_h	N_h	N_h
FIFIR	$N_1+N_2+N_g-2$	$N_1+N_2+N_g$	N_1+N_2	N_1+N_2

simultaneously by two filters: $\mathbf{w}_1$ and $\mathbf{g}*\mathbf{w}_2^U$. It seems that there are $(S-1)$ redundant taps. As we will show later, this is indeed the case, and the $(S-1)$ redundant taps will slow down the convergence rate of the proposed echo canceller. An easy and efficient way to overcome this problem is to null the redundant taps of $\mathbf{w}_1$; we let the coefficients $[w_{1,N_1-(S-1)M}\ \cdots\ w_{1,N_1-2M}\ w_{1,N_1-M}]$ all be zeros. This nulling scheme removes the redundant taps and accelerates the convergence rate.

To obtain the tap weights of $\mathbf{w}_1$ and $\mathbf{w}_2$, an adaptive algorithm is applied. From (4), we can see that the proposed echo cancellation filter, similar to a conventional FIR filter, has a linear structure. As a result, adaptive algorithms developed for the conventional FIR filter can be directly applied here. For the complexity consideration, the simplest adaptive algorithm, namely, the least mean square (LMS), is employed. The LMS algorithm is given by [9]

$$\mathbf{w}_{k+1}=\mathbf{w}_k+\mu e_k\tilde{\mathbf{x}}_k \tag{6}$$

where μ is the step size controlling the convergence rate, and $e_k=y_k-\tilde{y}_k$ is the error signal. In spite of the joint input vector, the above equation is identical to a typical LMS weights update equation for a transversal FIR filter. Hereafter, for the sake of convenience, we will call the proposed echo canceller the FIFIR echo canceller.

The computational complexity of the adaptive FIFIR echo canceller can be easily evaluated. Table I summarizes the numbers of additions and multiplications required in the echo cancellation for an FIFIR and a conventional FIR filter. As we can see, the complexity reduction for the proposed structure comes from the IFIR filter. The computational complexity of $\mathbf{w}_2$ is only one Mth of that of the corresponding FIR filter. Consider the SHDSL application studied in Section IV. The echo response length is 250, and the cutting point is set as 31. For interpolation factor 2, 4, and 8, the complexity reduction ratios over a conventional FIR filter are 63%, 45%, and 40%, respectively.

Given α and M, the optimal $\mathbf{g}$ is an ideal lowpass filter with bandwidth π/M; however, its impulse response is an unrealizable infinite sinc function. A simple remedy is to multiply the sinc function by a finite length widnow. From extensive simulations, we found that a tunnable stopband attenuation window, such as a Chebyshev window, gives satisfactory results.

III. THEORETICAL ANALYSIS

In this section, we consider some theoretical aspects of the proposed FIFIR filter. First, we derive the optimal Wiener solution and the corresponding MMSE. Using these results, we calculate the ERLE bounds for the adaptive FIFIR echo canceller.

Define $\mathbf{x}_{2,k}=[x_{k-\alpha}\ x_{k-(\alpha+1)}\ \cdots\ x_{k-N_h+1}]^T$ as the input data for the interpolator. Then, $\tilde{\mathbf{x}}_{2,k}$ can be expressed as

$$\tilde{\mathbf{x}}_{2,k}=\mathbf{M}\mathbf{x}_{2,k} \tag{7}$$

where

$$\mathbf{M}=\begin{bmatrix}\mathbf{g}^T,\underbrace{0,\ldots,0}_{(N_2-1)M}\\ \underbrace{0,\ldots,0}_{M},\mathbf{g}^T,\underbrace{0,\ldots,0}_{(N_2-2)M}\\ \vdots\\ \underbrace{0,\ldots,0}_{(N_2-1)M},\mathbf{g}^T\end{bmatrix} \tag{8}$$

is an N_2-by-$(N_h-\alpha)$ matrix. Without loss of generality, we can always pad zeros in the original echo so that the length of $\mathbf{x}_{2,k}$ equals $[N_g+(N_2-1)M]$. From (3) and (7), we then have

$$\tilde{y}_k=\mathbf{w}_1^T\mathbf{x}_{1,k}+\mathbf{w}_2^T\mathbf{M}\mathbf{x}_{2,k}. \tag{9}$$

The input vector of the FIFIR filter consists of $\mathbf{x}_{1,k}$ and $\tilde{\mathbf{x}}_{2,k}$. The vector $\mathbf{x}_{1,k}$ is typically white; however, $\tilde{\mathbf{x}}_{2,k}$ is not. The signal $\tilde{x}_k$ is the output from the interpolation filter $\mathbf{g}$. To simplify our analysis, we assume that $\mathbf{g}$ is an ideal lowpass filter. In other words, the frequency response of $\mathbf{g}$ is flat in the desired passband π/M. In this case, $\tilde{\mathbf{x}}_{2,k}$ is a white vector. With this assumption, the FIFIR echo canceller is identical to a conventional FIR echo canceller. The mean-squared error (MSE) criterion is then given as

$$J=E\left[(y_k-\tilde{y}_k)^2\right]. \tag{10}$$

If we take the derivative with respect to $\mathbf{w}$ and set the result to zero, we can obtain the Wiener solution of the FIFIR filter $\mathbf{w}_o$ as

$$\mathbf{w}_o=\mathbf{R}^{-1}\mathbf{p} \tag{11}$$

where $\mathbf{R}=E[\tilde{\mathbf{x}}_k\tilde{\mathbf{x}}_k^T]$ is the input correlation matrix, and $\mathbf{p}=E[\tilde{\mathbf{x}}_k y_k]$ is a cross correlation vector.

Next, we find closed-form expressions for $\mathbf{R}$ and $\mathbf{p}$. The correlation matrix can be rewritten as

$$\begin{aligned}\mathbf{R}&=E\left[\tilde{\mathbf{x}}_k\tilde{\mathbf{x}}_k^T\right]\\&=\begin{bmatrix}\mathbf{R}_{\mathbf{x}_1\mathbf{x}_1}&\mathbf{R}_{\mathbf{x}_1\tilde{\mathbf{x}}_2}\\ \mathbf{R}_{\mathbf{x}_1\tilde{\mathbf{x}}_2}^T&\mathbf{R}_{\tilde{\mathbf{x}}_2\tilde{\mathbf{x}}_2}\end{bmatrix}.\end{aligned} \tag{12}$$

Note that x_k is usually white. Thus

$$\begin{aligned}\mathbf{R}_{\mathbf{x}_1\mathbf{x}_1}&=E\left\{\mathbf{x}_{1,k}\mathbf{x}_{1,k}^T\right\}\\&=\sigma_x^2\mathbf{I}_{N_1\times N_1}\end{aligned} \tag{13}$$

where σ_x^2 is the transmitted signal variance. From (7), the correlation matrix is

$$\begin{aligned}\mathbf{R}_{\tilde{\mathbf{x}}_2\tilde{\mathbf{x}}_2}&=E\left\{\tilde{\mathbf{x}}_{2,k}\tilde{\mathbf{x}}_{2,k}^T\right\}\\&=E\left\{\mathbf{M}\mathbf{x}_{2,k}\mathbf{x}_{2,k}^T\mathbf{M}^T\right\}\\&=\sigma_x^2\mathbf{M}\mathbf{M}^T\end{aligned} \tag{14}$$

where $\mathbf{M}$ is the interpolation matrix in (8). The cross correlation matrix is

$$\begin{aligned}\mathbf{R}_{\mathbf{x}_1\tilde{\mathbf{x}}_2} &= E\left\{\mathbf{x}_{1,k}\tilde{\mathbf{x}}_{2,k}^T\right\} \\ &= E\left\{\mathbf{x}_{1,k}\mathbf{x}_{2,k}^T\mathbf{M}^T\right\} \\ &= \sigma_x^2\begin{bmatrix}\mathbf{0}_{\alpha\times N_o} & \mathbf{0}_{\alpha\times(N_h-N_1)} \\ \mathbf{I}_{N_o\times N_o} & \mathbf{0}_{N_o\times(N_h-N_1)}\end{bmatrix}\mathbf{M}^T. \end{aligned} \tag{15}$$

If we assume that noise n_k is independent of the transmitted signal x_k, then the cross correlation vector is

$$\begin{aligned}\mathbf{p} &= E\{\tilde{\mathbf{x}}_k y_k\} \\ &= E\left\{\begin{bmatrix}\mathbf{x}_{1,k} \\ \mathbf{M}\mathbf{x}_{2,k}\end{bmatrix}(\mathbf{h}^T\mathbf{x}_k + n_k)\right\} \\ &= \sigma_x^2\begin{bmatrix}\mathbf{h}(0:N_1-1) \\ \mathbf{M}\mathbf{h}(\alpha:N_h-1)\end{bmatrix}\end{aligned} \tag{16}$$

where the notation $\mathbf{h}(i:j)$ denotes a vector whose elements consisting of the ith to the jth component of $\mathbf{h}$.

To obtain the Wiener solution without redundant taps in $\mathbf{w}_1$, we must eliminate the ith row and ith column of $\mathbf{R}$, as well as the ith row of $\mathbf{p}$, where $i \in \{(N_1-(S-1)M),\cdots,(N_1-2M),(N_1-M)\}$. By doing so, the corresponding weights in $\mathbf{w}_1$ will be all zeros, i.e., $[w_{1,N_1-(S-1)M}\ \cdots\ w_{1,N_1-2M}\ w_{1,N_1-M}] = \mathbf{0}_{1\times(S-1)}$. Then, the Wiener solution with coefficient nulling can be solved by

$$\hat{\mathbf{w}}_o = \hat{\mathbf{R}}^{-1}\hat{\mathbf{p}} \tag{17}$$

where $\hat{\mathbf{R}}$ and $\hat{\mathbf{p}}$ are the correlation matrix and vector for the nulled filter, respectively. Using (11) or (17), we now are ready to derive the corresponding MMSE and ERLE.

The residual echo response is given by

$$\Delta\mathbf{h} = \mathbf{h} - \left(\mathbf{w}_{o,1} + \mathbf{g} * \mathbf{w}_{o,2}^U\right) \tag{18}$$

where $\mathbf{w}_{o,1}$ and $\mathbf{w}_{o,2}$ are the optimal weights for $\mathbf{w}_1$ and $\mathbf{w}_2$, respectively, and $\mathbf{w}_{o,2}^U$ is an upsampled version of $\mathbf{w}_{o,2}$. The MMSE is then equal to the summation of the residual echo power and the noise variance.

$$\text{MMSE} = (\Delta\mathbf{h}^T\Delta\mathbf{h})\sigma_x^2 + \sigma_n^2 \tag{19}$$

where σ_n^2 is the noise variance. The theoretical ERLE equals

$$\text{ERLE} = 10\cdot\log_{10}\frac{\mathbf{h}^T\mathbf{h}}{\Delta\mathbf{h}^T\Delta\mathbf{h}}. \tag{20}$$

So far, we have obtained two Wiener solutions for two adaptive FIFIR echo cancellers. We are then concerned with which one will be better. Although a theoretical comparison is not available, we have obtain the following results using extensive simulations. We found that the ERLEs for these two cancellers are almost the same; however, the eigenvalue spreads for two input correlation matrices are significantly different. The eigenvalue spread is defined as $\lambda_{\max}/\lambda_{\min}$, where $\lambda_{\max}$ and $\lambda_{\min}$ are the maximum and the minimum eigenvalues of an input correlation matrix. The eigenvalue spread of $\mathbf{R}$ is usually much larger than that of $\hat{\mathbf{R}}$. It is well known that the convergence rate of an adaptive algorithm is inversely proportional to the eigenvalue spread, which means that the convergence rate of the adaptive echo canceller without nulling will be much slower. Thus, we will use the one with nulling as the proposed echo canceller.

IV. Simulation Results

To test the robustness of our FIFIR echo canceller, we used eight CSA loops in [3] for simulations. We considered an SHDSL application where the sampling rate was as high as 775 KHz. The simulated echo responses at the central office side (CO) and the customer premise side (CPE) are shown in Fig. 4. The line code of the transmit signal was 16-PAM. Here, AWGN with -140 dBm/Hz was used to contaminate the received signal. The cutting point α was set at 31, and the interpolation factor M was set at 4. A Chebyshev windowed sinc function [11] with 23-tap was selected as the interpolation filter. We then have $N_1 = 50$. During the training period, the far-end transmit signal was turned off. After that, the transceiver was operated in a full duplex data transmission mode. For a faster convergence, the LMS algorithm with a variable step size was applied. The training period was divided into five stages, and the overall period was 12 000 samples. In each stage, the step size was reduced by a factor of two. The emulated echo response, which was an overlapped combination of the FIR and IFIR responses, is shown in Fig. 5 for CSA loop # 1. Note that there was two nulled taps (zero weights) located in the tail end of $\mathbf{w}_1$. As we can see, the tail response was modeled accurately using the IFIR, except for the transient response in the beginning; however, $\mathbf{w}_1$ compensated for that effectively.

All eight CSA test loops, both at the CO and the CPE side, were simulated. The resultant ERLE performances are shown in Fig. 6. As

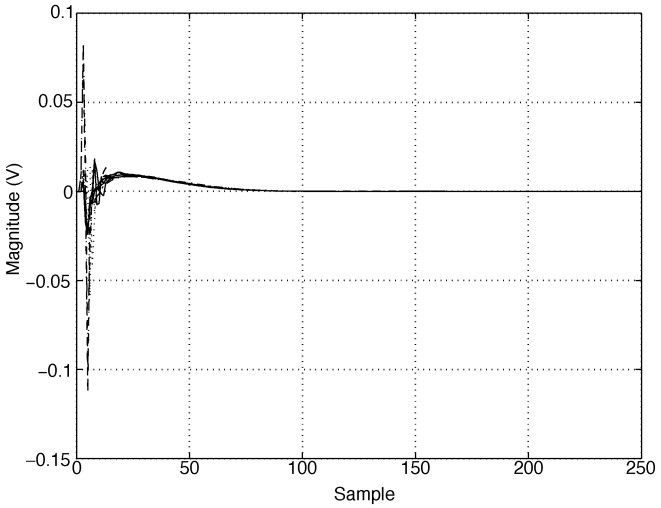

Fig. 4. SHDSL echo responses for CSA loops at CO and CPE side.

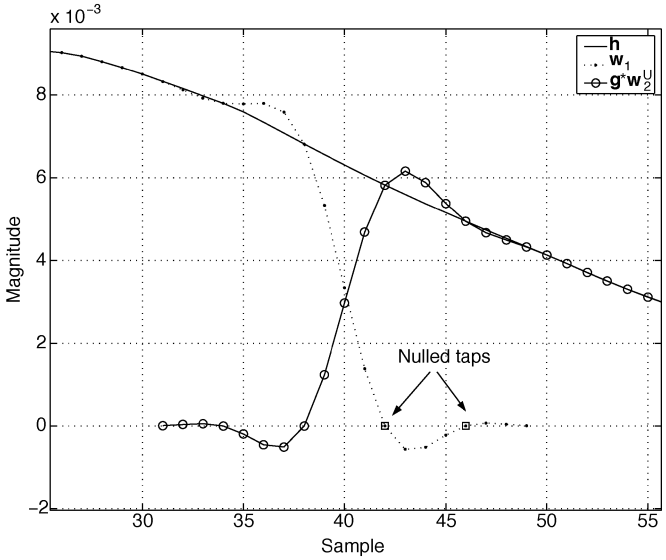

Fig. 5. Overlapping of FIR and IFIR filters ($M = 4$, $S = 3$, $N_1 = 50$).

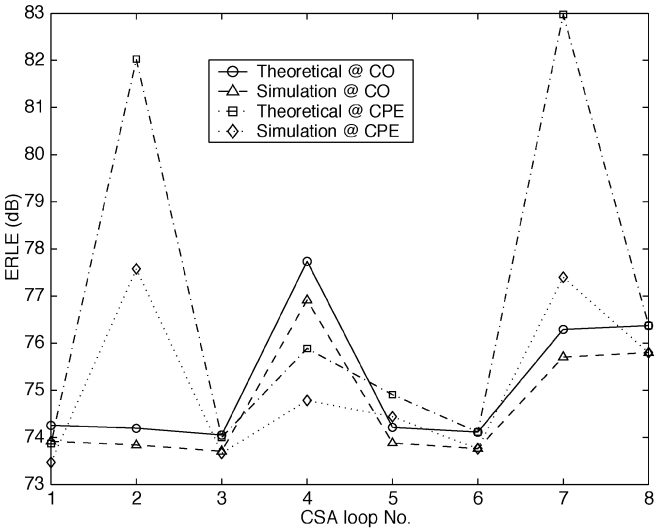

Fig. 6. ERLE performance for different CSA loops.

the figure shows, the ERLE was between 73.4 and 77.5 dB. The averaged ERLE was around 74.7 dB at the CO side and 75.1 dB at the CPE side. These ERLE results exceed the general requirement for a DSL echo canceller (60–70 dB). The low sensitivity of the proposed echo canceller to different topologies and loop characteristics exhibited its feasibility to real-world applications. Generally speaking, theoretical ERLE predictions, which are also shown in Fig. 6, were accurate. The higher the ERLE, the larger the difference between the theoretical and empirical ERLEs. This was because if the ERLE was higher, a smaller step size was required to hold the independence theory. However, we used the same step size for all cases.

V. Conclusions

A low-complexity, finite impulse response, and adaptive filter structure is proposed for the echo cancellation application in high-speed baseband xDSL systems. The proposed echo canceller is a generalized adaptive interpolated FIR structure. It inherits all the numerical stability advantages of the conventional FIR filter while effectively reducing its computational complexity. Using the proposed tap-weight overlapping and nulling scheme, the performance loss due to the uncontrollable transient response problem was avoided. The theoretical performance bounds for the proposed echo canceller were also derived and verified. Finally, simulations using standard test loops were conducted to demonstrate the effectiveness of the proposed echo canceller.

References

[1] W. Y. Chen, J. L. Dixon, and D. L. Waring, "High bit rate digital subscriber line echo cancellation," *IEEE J. Select. Areas Commun.*, vol. 9, pp. 848–860, Aug. 1991.

[2] High Bit-Rate Digital Subscriber Line (HDSL) Transmission System on Metallic Local Lines. ETSI TS 101 135, Sept. 2000.

[3] High Bit Rate Digital Subscriber Line—2nd Generation (HDSL2): ANSI T1.418, 2002.

[4] Single-Pair High-Speed Digital Subscriber Line (SHDSL) Transceivers: ITU-T Rec. G.991.2, Feb. 2001.

[5] A. N. Kaelin, A. G. Lindgren, and G. S. Moschytz, "Simplified adaptive IIR filters based on optimized orthogonal prefiltering," *IEEE Trans. Circuits Syst.*, vol. 42, pp. 326–333, May 1995.

[6] G. W. Davidson and D. D. Falconer, "Reduced complexity echo cancellation using orthonormal functions," *IEEE Trans. Circuits Syst.*, vol. 38, pp. 20–28, Jan. 1991.

[7] A. Abousaada, T. Aboulnasr, and W. Steenaart, "An echo tail canceller based on adaptive interpolated FIR filtering," *IEEE Trans. Circuits Syst. II*, vol. 39, pp. 409–416, July 1992.

[8] Y. Neuvo, C. Y. Dong, and S. K. Mitra, "Interpolated finite impulse response filters," *IEEE Trans. Acoust. Speech, Signal, Processing*, vol. ASSP-32, pp. 563–570, June 1984.

[9] S. Haykin, *Adaptive Filter Theory*. Englewood Cliffs: Prentice-Hall, 1991, ch. 9.

[10] T. Starr, J. M. Cioffi, and P. Silverman, *Understanding Digital Subscriber Line Technology*. Englewood Cliffs, NJ: Prentice-Hall, 1998, ch. 3.

[11] S. S. Lin and W. R. Wu, "A low complexity adaptive interpolated FIR echo canceller," in *Proc. IEEE ISCAS*, May 2001.